Catalysis Today 160 (2011) 165–169

Contents lists available at ScienceDirect

Catalysis Today

journal homepage: www.elsevier.com/locate/cattod

The location of gold nanoparticles on titania: A study by high resolution aberration-corrected electron microscopy and 3D electron tomography

Juan C. Hernández-Garrido[a,b], Kenta Yoshida[c,d], Pratibha L. Gai[c,d], Edward D. Boyes[c,d], Claus H. Christensen[e], Paul A. Midgley[a,*]

[a] Department of Materials Science and Metallurgy, University of Cambridge, Pemboke Street, Cambridge CB2 3QZ, UK
[b] Facultad de Ciencias, Universidad de Cadiz, Campus Rio San Pedro, ES-11510 Puerto Real, Cadiz, Spain
[c] The Nanocentre, Department of Chemistry, The University of York, York YO10 5DD, UK
[d] The Nanocentre, Department of Physics, The University of York, York YO10 5DD, UK
[e] Haldor Topsøe A/S, Nymøllevej 55, 2800 Kgs. Lyngby, Denmark

ARTICLE INFO

Article history:
Available online 15 July 2010

Keywords:
Gold nanoparticles
3D analysis
Titania
Electron tomography
Aberration-corrected electron microscopy
Heterogeneous catalysts

ABSTRACT

Using HAADF-STEM electron tomography and aberration-corrected TEM/STEM electron microscopy, 3D reconstructions and high resolution images have been recorded of heterogeneous catalysts consisting of gold nanoparticles supported on titanium dioxide (anatase); these catalysts have gained attention recently because of their potential for use in many reactions with both industrial and environmental importance. We will illustrate how through the combination of high resolution images and segmented 3D tomographic data, structural features of the supported phase can be revealed which are normally not accessible through conventional imaging. The location of the nanoparticles preferentially at the grain boundaries, confirmed by these studies, is likely to influence the stability of the nanoparticles and is a key step in understanding and facilitating the development of better catalysts.

1. Introduction

In recent years, gold catalysts have received a great deal of attention because of their potential for many reactions of both industrial and environmental importance [1]. Gold was widely believed to be a catalytically inactive material for a long time but this situation changed dramatically with the discovery of the catalytic activity of gold nanoparticles [2,3].

The remarkable catalytic properties of supported gold were first shown through the oxidation of CO at sub-ambient temperature by Haruta et al. [4]. In recent years the most studied catalyst for preferential oxidation of CO in a H_2 stream has been gold supported on titania: for this reaction Au/TiO_2 is one of the most active catalysts at low temperatures [5,6] and the optimum gold nanoparticle size was found to be ca. 3 nm. Studies on gold catalysts show that macroscopic gold is only weakly active for CO oxidation but Au in nano-dispersed form, with strong metal–support interaction, leads to highly active catalysts [7,8]. The so-called strong metal–support interaction (SMSI) is often seen as critical to sustaining high catalytic activity under demanding catalyst operation conditions (i.e. high temperature, high water vapour pressure, etc.). Indeed, SMSI has been linked directly to the presence of electronic defects that can be prepared with ease on the surface of reducible oxides (e.g., CeO_2 and TiO_2) [8]. The possibility of anchoring these active metal components to these electronic defects has been documented [9,10], with strong interaction between the active metal and defects of reducible oxides fundamentally determining the dispersion, morphology and, therefore, the catalytic activity of metal clusters.

The firmly established fact that gold nanoparticles function as highly active catalysts [5,8,11] has given rise to much speculation and theoretical analysis [10,12] as to the root cause of this phenomenon. It seems likely that atoms of gold that are situated at the periphery of a nanoparticle are the foci of catalytic activity principally because of their low coordination number [11]. Density-functional theory (DFT) calculations of Nørskov et al. [12] point strongly to this interpretation, and has prompted further investigation as to the origins of enhanced catalytic activity in nanoparticle gold as well as other metals including bimetallic entities.

However the detailed nanostructure and the location of the nanoparticles in the Au/TiO_2 system at the atomic scale, which could be vital for catalytic activity, selectivity and the nanoparticle stability, are not well understood and a number of recent studies have been carried out dealing with this investigation, primarily using electron microscopy [13].

* Corresponding author. Tel.: +44 1223 334561; fax: +44 1223 334563.
E-mail address: pam33@cam.ac.uk (P.A. Midgley).

0920-5861/$ – see front matter © 2010 Elsevier B.V. All rights reserved.
doi:10.1016/j.cattod.2010.06.010

These physicochemical data can in general be validated by transmission electron microscopy. However, interpretation of conventional electron micrographs can often be ambiguous because only 2D projections of the objects are recorded. In this sense, electron tomography has proven to be a powerful tool to enable a more complete 3D characterization of heterogeneous catalysts and particularly of supported metal catalysts [14–16]. Of all the possible imaging modes available for electron tomography, those based on high angle annular dark field (HAADF) imaging in the scanning transmission electron microscope (STEM) are the most suited to reveal the 3D structure of crystalline nanomaterials and are particularly useful in studies of supported nanoparticle catalysts. The high angle annular dark field detector collects electrons that undergo Rutherford scattering and the intensity of such images, approximately proportional to Z^2 (where Z is the atomic number of the scattering atom), make it ideal for the investigation of heterogeneous materials with components of very different atomic numbers present [17].

In this work, to obtain a better insight into the atomic structure and location of the gold nanoparticles on the support, we have investigated the fine structure of the catalysts directly using aberration-corrected (AC) TEM and HAADF-STEM combined with three-dimensional characterization using HAADF-STEM electron tomography.

2. Experimental

The nanostructures of the sample were imaged in a JEOL 2200FS double aberration-corrected TEM/STEM, operating at 200 kV, in the York JEOL Nanocentre at the University of York [18]. Both TEM and high angle annular dark field STEM (HAADF-STEM) were carried out in the AC-TEM/STEM. The dual aberration-correctors in AC-TEM and AC-HAADF-STEM imaging of the supported nanocatalyst sample provide insights into the atomic level structure critical to understanding the reactivity properties of nanocatalysts. Low electron dose imaging was used throughout.

Electron tomography experiments were performed on a FEI Tecnai F20 field-emission gun scanning transmission electron microscope operated at 200 kV at the University of Cambridge. Data collection was performed by tilting the specimen about a single axis using a Fischione ultrahigh-tilt tomography holder, ranging from −72° to +68° in steps of 2°. Image acquisition was undertaken using the FEI software package Xplore3D. Alignment of the image stack and tomographic reconstructions were performed with the FEI software package Inspect 3D using the iterative routine SIRT. Surface rendering, after a manual segmentation process, was undertaken using Amira software.

3. Results and discussion

Fig. 1 shows a typical AC-TEM image of Au/TiO_2 catalysts. Small gold nanoparticles with an average particle size of 2.0 nm are shown supported by crystallites of TiO_2. Structural analysis indicates that the lattice spacings for the support correspond to the anatase form of titania, as indicated in Fig. 2 where a lattice spacing d = 0.35 nm, corresponding to the (1 0 1) lattice planes for the anatase, is identified.

A closer view for the exposed surface (Fig. 2) of the support crystallites indicates a high degree of roughness. This high resolution lattice image has been recorded slightly underfocus to enhance the phase contrast at the edge of the sample (Fresnel contrast). That allows a better visualization of any surface roughness and here we estimate a surface roughness of about 1 nm, determined using successive anatase (1 0 1) planes assigned in the figure (i), (ii) and (iii).

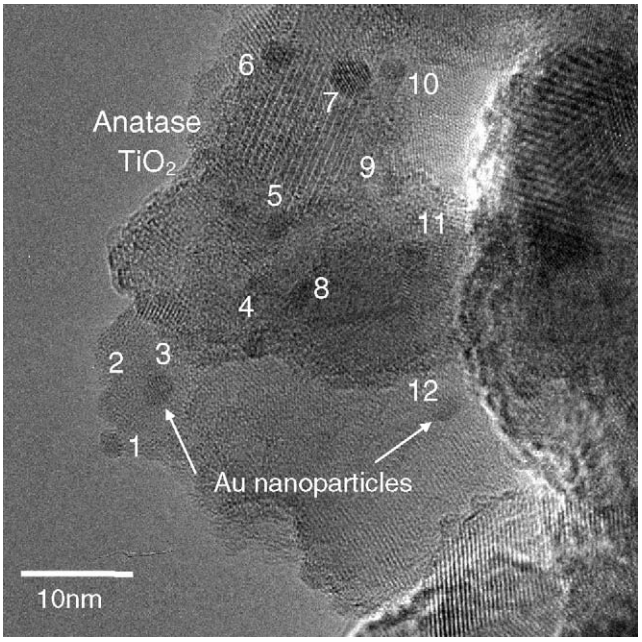

Fig. 1. AC-TEM image of Au nanoparticles (labeled 1–12, with average diameter 2 nm) supported on anatase TiO_2. There is some evidence that the particles are preferentially located at grain boundaries.

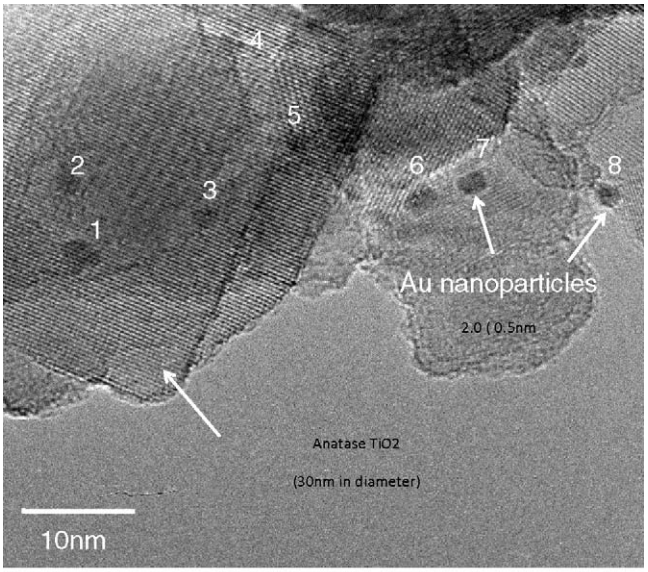

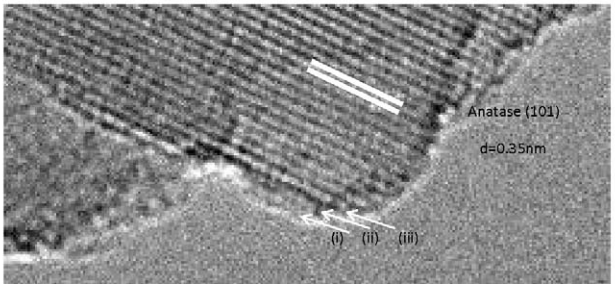

Fig. 2. (Top) AC-TEM image of Au nanoparticles (labeled 1–8, with average diameter of 2 nm) supported on anatase TiO_2. Large (30 nm) plate-like crystals of anatase are visible. The roughness of the crystal surface is more evident. (Bottom) An enlarged part of the image above showing in more detail the roughness of the crystal edge, equivalent to approximately three (1 0 1) planes or ca. 1 nm.

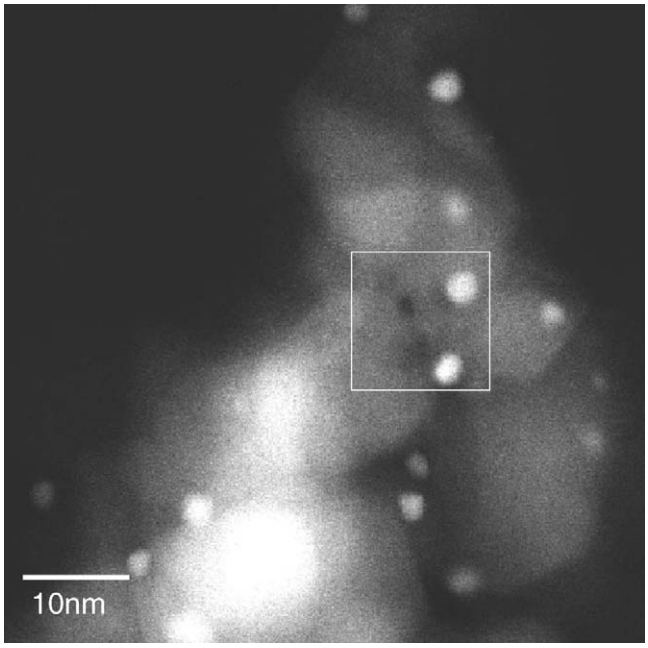

Fig. 3. AC-HAADF-STEM image of Au nanoparticles on titania. The atomic number contrast is evident with the Au nanoparticles standing out easily on the lighter support. Regions of titania which are thick in projection are also of high intensity. This image indicates a possible preference of Au nanoparticles to be located at grain boundaries.

The high resolution AC-HAADF-STEM (*Z*-contrast) image of Fig. 3 suggests strongly that the gold nanoparticles are located preferentially at the grain boundaries of the titania grains. Fig. 4 shows an enlarged part of Fig. 3 highlighting the {1 1 1} planes of the Au nanoparticles and, in the high-pass filtered version, illustrates the different titania grain orientations at the atomic level. The boundary in this image is composed of (2 0 0) and (0 0 4) anatase planes; the gold nanoparticles are located very near to the boundary.

To better understand and confirm the observations obtained by the AC-TEM/STEM studies, electron tomography was used to obtain a three-dimensional view of the Au/titania structure and relationship.

Fig. 5(left) shows a HAADF-STEM image acquired as part of the tomographic tilt series. In this image the gold nanoparticles seem to be distributed over the TiO_2 nano-crystallites without any obvious preferential location at edges, faces or grain boundaries. The advantages to using 3D characterization become apparent when we compare this 2D image with the 3D reconstruction.

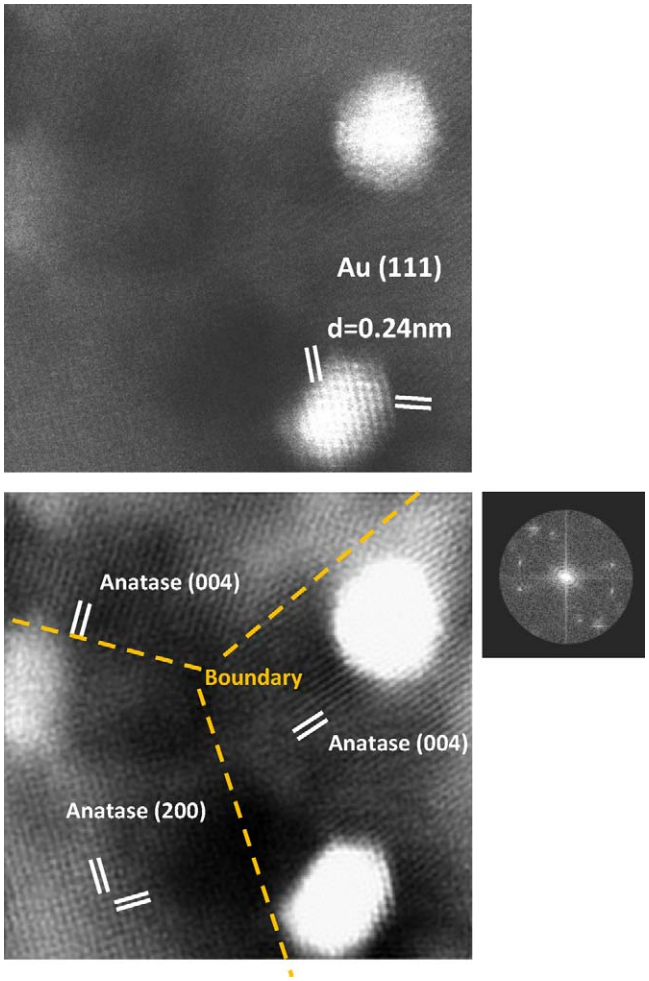

Fig. 4. (Top) An enlarged part of Fig. 3 (boxed region) showing two Au nanoparticles. The Au lattice fringes correspond to {1 1 1} planes. The titania lattice is just visible. (Bottom) Using a high-pass filter, illustrated in the inset Fourier transform, the titania lattice fringes can be made more visible. This allows the titania grain boundaries to be seen more clearly (shown as orange dashes). (For interpretation of the references to color in this figure legend, the reader is referred to the web version of this article.)

Fig. 5(center) shows a surface-rendered representation of the segmented 3D reconstructed volume of the catalyst. The two images in Fig. 5 are oriented such that a direct comparison can be made. The small volumes, colored red in the figure, correspond to the

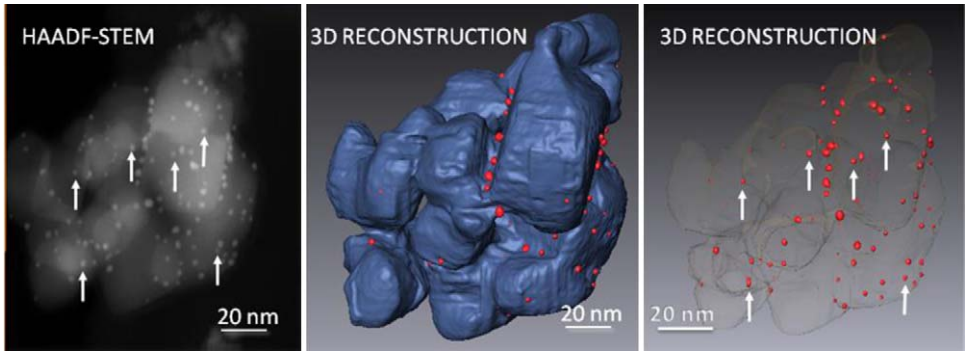

Fig. 5. (Left) 2D HAADF image from the tilt series acquired for the tomographic reconstruction. (Center) Surface-rendered representation of the segmented reconstruction of the Au/TiO_2 catalyst. Au particles are coloured red and the titania coloured blue. Note that most of the gold nanoparticles are located near the grain boundaries of the titania support crystallites. (Right) Surface-rendered partially transparent representation of the TiO_2 with all the reconstructed metallic nanoparticles shown. Arrows are included as a guide to the eye to show that some nanoparticles not visualized in the center figure are because they lie behind the support crystallites as seen in this viewing direction. (For interpretation of the references to color in this figure legend, the reader is referred to the web version of this article.)

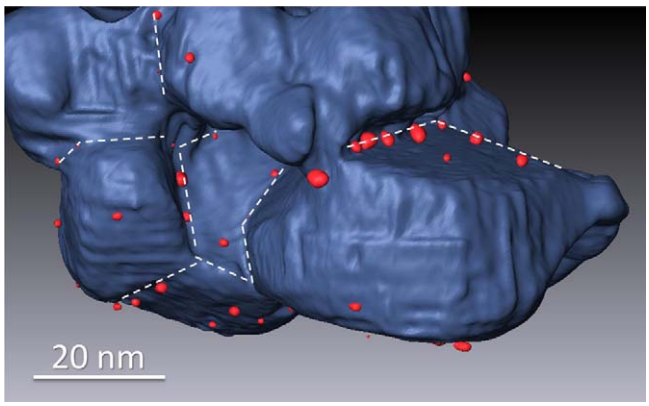

Fig. 6. Magnified region showing the distribution of gold nanoparticles in the 3D reconstruction of the Au/TiO_2 catalyst. Note the aligned distribution of the metal particles along the boundaries between supporting crystallites.

gold nanoparticles; particles with diameters in the range 1–3 nm have been successfully segmented from the reconstruction. The regions in blue correspond to the anatase support. Fig. 5(right) illustrates how many nanoparticles (examples are arrowed) are missed in the center figure because they lie behind the supporting titania crystallite as viewed in this direction.

The location of gold nanoparticles can be determined reliably from the 3D reconstruction. As seen from Fig. 5 most of the metal particles appear to be located at the titania grain boundaries. Fig. 6 is a magnified region of the surface-rendered reconstructed volume showing the distribution of gold nanoparticles aligned along the boundaries between supporting crystallites. Dashed lines are included as a guide for the eye. It is clear from the reconstruction that remarkably few metal nanoparticles are located on the facets themselves, instead preferring facet vertices and boundaries. Another feature that can be seen from these surface-rendered images is the high degree of roughness at the TiO_2 surface, qualitatively in agreement with the AC-TEM images.

Fig. 7 shows a single *XY* orthoslice taken from the 3D reconstructed volume. The orthoslice provides an additional imaging tool to study the location of the gold nanoparticles; here the nanoparticles correspond to the high intensity areas seen in the orthoslice, some of which are indicated by arrows as a guide to the eye. The preferential location of nanoparticles on facet vertices and nanocrystal boundaries is clear. The horizontal streaking seen in the figure is a result of reconstruction artefacts resulting from the limited tilt range and number of images coupled with the localized high contrast of the nanoparticles.

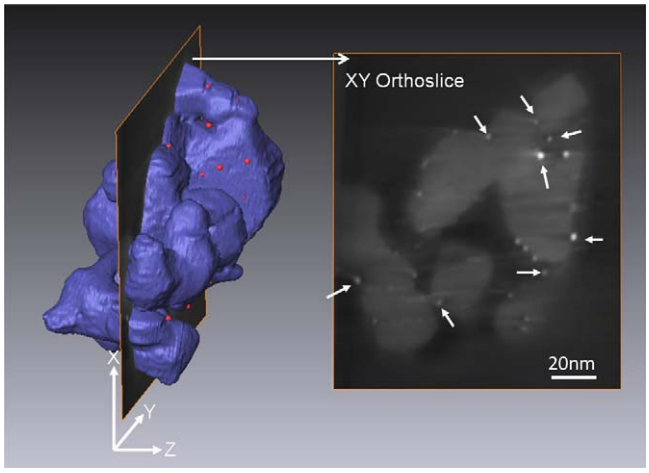

Fig. 7. An *XY* orthoslice taken from the 3D reconstructed volume taken perpendicular to the *Z*-direction. The arrows indicate the location of the Au nanoparticles on facet vertices and grain boundaries of the titania support crystallites.

4. Conclusions

It is generally accepted that the catalytic activity and selectivity of gold catalysts supported on TiO_2 are determined to a large extent by the Au/TiO_2 interface, possible Au/TiO_2 charge transfer, and the size and shape of the nanoparticles. The stabilization of the gold nanoparticles by the metal oxide clearly plays an important role and the correct choice of support appears to help distribute the gold particles across the surface and perhaps by means of strong metal–support interactions, prevents unwanted coalescence.

Although there is now a body of knowledge regarding the catalytic activity and selectivity for Au/TiO_2 catalysts, until recently there has been little information available about the 3D spatial distribution of these highly active nanoparticles over the support; in terms of catalysis, the accessibility of the supported nanoparticles to reactant molecules is determined by their location with respect to the support surface. As has been described elsewhere by some of us [13] for a similar catalytic system, in terms of stabilization the contribution of interface energy to the total energy of these small particles is expected to be important. It can be demonstrated that for a particle with a given size, there is a notable increment in the interface contact area between a situations on a flat surface to another one in which the particle sits on a nanocrystal boundary. This interface energy effect could clearly contribute to the stabilization of the gold nanoparticles over the titania support.

Our study shows that gold nanoparticles show a strong preference to be located at the titania grain boundaries and vertices and regions which show high surface roughness. A structural relationship between the metal and the underlying oxide support may be responsible for the predominance of this feature.

These observations have been made using a combination of electron tomography and aberration-corrected TEM/STEM and together is shown to be a powerful tool for the characterization of size, structure and distribution of active nanoparticles on a support. Information such as that provided in this work may play an important role in the development and design of new nanomaterials with desired catalytic properties.

Acknowledgments

Sir John Meurig Thomas is kindly acknowledged for stimulating discussions. J.C.H.G. and P.A.M. acknowledge financial support from the European Union under the Framework 6 program for an Integrated Infrastructure Initiative, Ref.: 026019 ESTEEM. P.L.G., K.Y. and E.D.B. thank University of York, Yorkshire Forward/EU and JEOL, for sponsoring the York JEOL Nanocentre, including the double aberration-corrected JEOL 2200FS TEM/STEM instrument.

References

[1] C.H. Christensen, J.K. Nørskov, Science 327 (2010) 278–279.
[2] M. Haruta, S. Tsubota, T. Kobayashi, H. Kageyama, M.J. Genet, B. Delmon, J. Catal. 144 (1993) 175–192.
[3] M. Haruta, Catal. Today 36 (1997) 153–166.
[4] M. Haruta, T. Kobayashi, H. Sano, N. Yamada, Chem. Lett. 2 (1987) 405–408.
[5] T.V.W. Janssens, B.S. Clausen, B. Hvolbæk, H. Falsig, C.H. Christensen, T. Bligaard, J.K. Nørskov, Top. Catal. 44 (2007) 15–26.
[6] J.-D. Grunwaldt, A. Baiker, J. Phys. Chem. B 103 (1999) 1002–1012.
[7] V. Malden, X. Lai, D.W. Goodman, Science 281 (1998) 1647–1650.
[8] S.J. Tauster, S.C. Fung, R.T.K. Baker, J.A. Horsley, Science 211 (1981) 1121–1125.
[9] N. Lopez, J.K. Nørskov, T.V.W. Janssens, A. Carlsson, A. Puig-Molina, B.S. Clausen, J.-D. Grunwaldt, J. Catal. 225 (2004) 86–94.
[10] M.S. Chen, D.W. Goodman, Science 306 (2004) 252–255.

[11] P.P. Edwards, J.M. Thomas, Angew. Chem. Int. Ed. 46 (2007) 5480–5486.
[12] N. Lopez, J.K. Nørskov, JACS 124 (2002) 11262–11263.
[13] J.C. Gonzalez, J.C. Hernández, M. López-Haro, E. del Río, J.J. Delgado, A.B. Hungría, S. Trasobares, S. Bernal, P.A. Midgley, J.J. Calvino, Angew. Chem. Int. Ed. 48 (2009) 5313–5315.
[14] E.P. Ward, T.J.V. Yates, J.-J. Fernández, D.E.W. Vaughan, P.A. Midgley, J. Phys. Chem. C 111 (2007) 11501–11505.
[15] A.H. Janssen, C.-M. Yang, Y. Wang, F. Schüth, A.J. Koster, K.P. de Jong, J. Phys. Chem. B 107 (2003) 10552–10556.
[16] P.A. Midgley, M. Weyland, J.M. Thomas, B.F.G. Johnson, Chem. Commun. 18 (2001) 907.
[17] J.M. Thomas, P.A. Midgley, T.J.V. Yates, J.S. Barnard, R. Raja, I. Arslan, M. Weyland, Angew. Chem. Int. Ed. 43 (2004) 6745–6747.
[18] P.L. Gai, E.D. Boyes, Microsc. Res. Tech. 72 (2009) 153.